Electronic Supplementary Material (ESI) for Reaction Chemistry & Engineering.

Playing with process conditions to increase the industrial sustainability of poly(lactic acid)-based materials

K. De Smit,[1] Y.W. Marien,[1] P.H.M. Van Steenberge,[1] D.R. D'hooge,[1,2*] M. Edeleva[3]

[1] Laboratory for Chemical Technology (LCT), Ghent University, Technologiepark 125, B-9052 Gent, Belgium.

[2] Centre for Textile Science and Engineering (CTSE), Ghent University, Technologiepark 70a, B-9052 Gent, Belgium.

[2] Centre for Polymer Materials and Technologies (CPMT), Ghent University, Technologiepark 70a, B-9052 Gent, Belgium.

Contents

S.1 Extra simulations for the results in the main text

Figure S1 shows an evolution of the *k*MC reaction rates for the β-scission and bimolecular mid-chain radical (MCR) termination. The colors correspond to the following conditions in the main text regarding Figure 7:red: 0.5m% BPO and green: 0.1m% BPO. It is clear that a higher peroxide concentration leads to a dominant termination reaction as the termination rate involves a second order radical concentration. The decrease in x_n for the lower BPO amounts seen in Figure 6 and Figure 7 in the main text is because the chain length decrease caused by β-scission is more important on a number basis, even though MCR termination has a similar reaction rate.

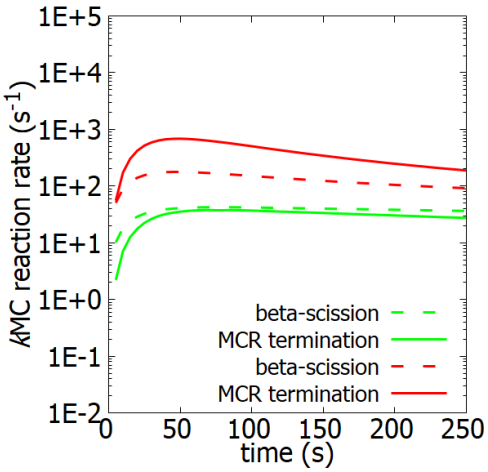

Figure S1: *k*MC reaction rates for β-scission (dotted lines) and MCR termination (full lines) for two conditions discussed in the main text Figure 8. Red: 0.5 m% BPO and green: 0.1 m% BPO.

Figure S2 shows the k_{diff} evolution for small-large (dotted lines) and large-large (full lines) molecule interactions during a simulation using the coupled parallel encounter pair model with free volume theory based parameters (green lines) or with RAFT-CLD-T parameters (red lines). It is clear that, overall, the utilization of FVT-based parameters results in lower values for k_{diff} but the difference between large-large and small-large behavior is more pronounced. The utilization of the RAFT-CLD-T parameters causes an underestimation of the diffusional limitations in a polymer modification environment as this model is not that able to correctly predict literature based experimental polymer properties (cf. discussion Figure 6)

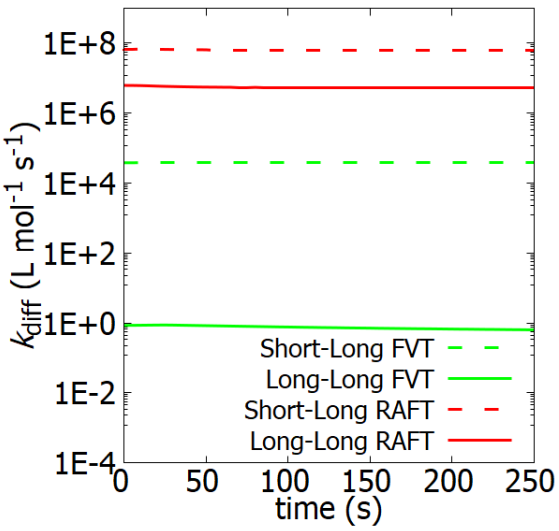

Figure S2: k_{diff}-values for small-large (dotted lines; involvement of crosslinking agent; CA) and large-large (full lines; termination with mid-chain radcials) molecule interactions during simulations using the coupled parallel encounter pair model (green lines) and the RAFT-CLD-T (red lines). Conditions of Figure 6b.

Figure S3 gives an evolution of *k*MC reaction rates during a PLA crosslinking simulation focusing on the CA addition reaction (red line), the crosslink reaction involving CA (orange line), β-scission of MCR's (green line) and MCR termination (blue line). It is clearly visible that small molecule-large molecules interactions such as the CA addition are favored at the start of the reaction. Due to the increase of CA-functionalized PLA chains, crosslinking (via a CA-aided crosslink pathway) becomes more likely than β-scission, explaining why the addition of CA results in a much higher increase of the average chain length in Figure 9 in the main text.

Figure S4 shows a histogram for the amount of crosslinks/branching points per chain for the same conditions that are discussed in Figure 7 in the main text. It is clear that increasing the peroxide concentration increases not only the amount of crosslinked/branched chains but also the quantity of crosslinks per chain. At higher peroxide concentrations (0.5m% and 1.0m%; orange and red rectangles) even chains with a backbone functionality of 6 or higher are formed. This indicates that the CMMC model is very able to track the intermolecular connectivity on a chain-by-chain basis.

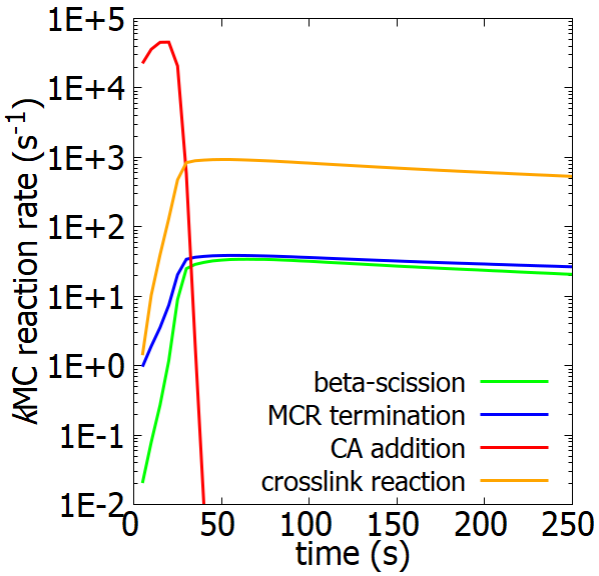

Figure S3: kMC reaction rates for β-scission (green full line), MCR termination (blue full line), CA addition (red full line) and the CA-aided crosslink reaction (orange full line); Conditions of Figure 6b.

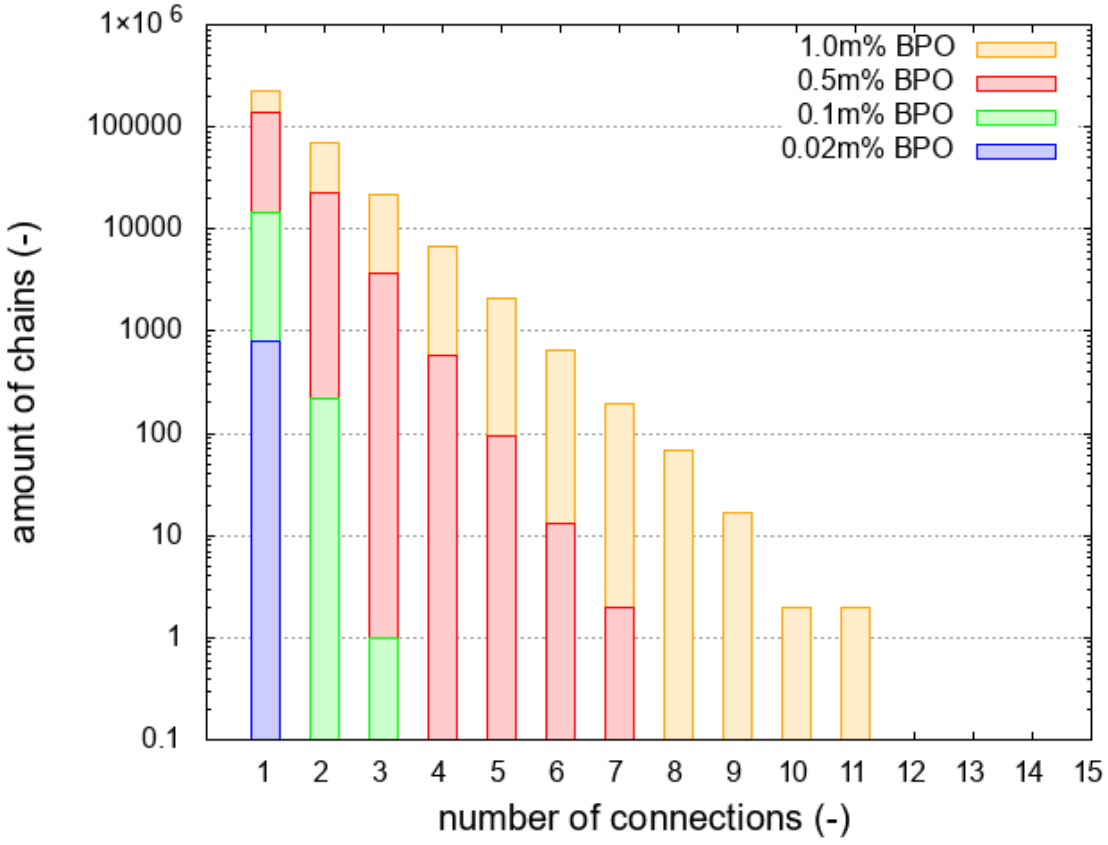

Figure S4: Histogram showing the amount of chains in the simulated ensemble containing a specific number of intermolecular connections (branching and crosslink points). Orange bars: 1.0m% BPO, red bars: 0.5m% BPO, green bars: 0.1m% BPO and blue bars: 0.02m% BPO; conditions of Figure 7.

S.2 Diffusional limitations

S.2.1 Diffusional limitations on peroxide dissociation

The evolution of the apparent initiator efficiency f_{app} with increasing monomer conversion is taken from the work of Buback *et al.*[1]:

$$f_{app} = \frac{D_I}{D_I + D_{term}} \qquad (S1)$$

in which D_I is the diffusion coefficient of the peroxide radical and D_{term} a correction factor, related to the rate of termination between two peroxide radicals. Buback only reported this value for 343K (5.3 10^{-10} $m^2 s^{-1}$). Since the present work focuses on polymer modification at very high temperature (463 K) we changed this value to 8.3 10^{-10} $m^2 s^{-1}$. The free volume theory is used to obtained D_I at a given temperature and reaction mixture composition:

$$D_I = D_{0,I}\, e^{-\frac{E_{a,I}}{RT}} e^{\left(-\frac{w_m V_m^* \xi_{cp}/\xi_{mp} + w_p V_p^* \xi_{cp}}{V_{FH}/\lambda}\right)} \qquad (S2)$$

$$\frac{V_{FH}}{\lambda} = \frac{K_{mm}}{\lambda} w_m \left(K_{mp} - T - T_{g1}\right) + \frac{k_{mp}}{\lambda}\, w_p \left(K_{pp} + T - T_{g1}\right) \qquad (S3)$$

with D_I the diffusion coefficient for the peroxide radical, $D_{0,I}$ the pre-exponential factor, $E_{a,I}$ the energy per mole that a cyanoisopropyl radical needs to overcome attractive forces which hold it to its neighbours, w_x the mass fraction of monomer ($x = m$) or polymer ($x = p$), V_x^* the specific volume of the monomer ($x = m$) or the polymer ($x = p$), ξ_{xy} the ratio of the critical molar volume of the peroxide radical ($x = c$) or monomer ($x = m$) compared to the polymer ($y = p$), and V_{FH}/λ related to the total free volume. Table S1 gives an overview of the related parameters (AIBN/(poly)styrene system but sufficiently representative).

Table S1: Parameters to enable the calculation of the apparent initiator efficiency[1,2].

Parameter	Description	Value[1,2]
$D_{0,I}\ (m^2 s^{-1})$	Pre-exponential factor for diffusion	$1.87\ 10^{-8}$
$E_I\ (kJ\ mol^{-1})$	Activation energy for diffusion	7.10 [(a)]
$R\ (J\ mol^{-1} K^{-1})$	Universal gas constant	8.314
$T\ (K)$	Temperature	$323 - 363$
$w_m\ (-)$	Mass fraction of monomer	0-1
$w_p\ (-)$	Mass fraction of polymer	0-1
$V_m^*\ (m^3 mol^{-1})$	Specific critical hole free volume of monomer	$0.822\ 10^{-6}$
$V_p^*\ (m^3 kg^{-1})$	Specific critical hole free volume of polystyrene	$0.77\ 10^{-6}$
$\frac{K_{mm}}{\lambda}\ (m^3\ kg^{-1}\ K^{-1})$	Parameter for specific hole free volume monomer	$1.49\ 10^{-9}$
$\frac{K_{mp}}{\lambda}\ (m^3\ kg^{-1}\ K^{-1})$	Parameter for specific hole free volume polymer	$5.82\ 10^{-10}$
$K_{pm} - T_{g1}\ (K)$	Parameter for specific hole free volume monomer	72.26
$K_{pp} - T_{g1}\ (K)$	Parameter for specific hole free volume polymer	-250.21
$\xi_{cp}\ (-)$	Critical jumping unit volume ratio for benzoyl peroxide radical to polymer	0.537
$\xi_{mp}\ (-)$	Critical jumping unit volume ratio for monomer to polymer	0.712

[(a)] values are slightly adjusted in order to improve description of experimental data.

S.2.2 Coupled parallel encounter pair model

a) Bimolecular to unimolecular reaction (as forward of the reversible):

$$A + B \underset{k_{-diff}}{\overset{k_{+diff}}{\rightleftharpoons}} AB \underset{k_{-chem*}}{\overset{k_{+chem*}}{\rightleftharpoons}} C \rightarrow A + B \underset{k_{-app}}{\overset{k_{+app}}{\rightleftharpoons}} C$$

Writing the mass balance for the species C and applying the quasi steady state assumption (QSSA) for the concentration of the encounter pair AB, it follows that:

$$\frac{1}{k_{-app}} = \frac{1}{k_{-chem}} + \frac{K_{eq}}{k_{+diff}} \qquad (S4)$$

$$\frac{1}{k_{+app}} = \frac{1}{k_{+chem}} + \frac{1}{k_{+diff}} \qquad (S5)$$

with K_{eq} being:

$$K_{eq} = \frac{k_{+chem*}}{k_{-chem*}} \frac{k_{+diff}}{k_{-diff}} = \frac{k_{+chem}}{k_{-chem}} \qquad (S6)$$

In Table S2, the Arrhenius parameters for releated k_{+chem} and k_{-chem} combinations are shown.

Table S2: Arrhenius parameters for k_{+chem} and k_{-chem}, bimolecular to unimolecular reactions[3–7].

Reaction	k_{+chem}		k_{-chem}	
	A	E_a	A	E_a
MCR-MCR termination	$9.0 \cdot 10^6$ L mol^{-1} s^{-1}	5.6 kJ mol^{-1}	$1.0 \cdot 10^{16}$ s^{-1}	280 kJ mol^{-1}
MCR-ECR termination	$4.2 \cdot 10^9$ L mol^{-1} s^{-1}	6.6 kJ mol^{-1}	$1.0 \cdot 10^{16}$ s^{-1}	280 kJ mol^{-1}
ECR-ECR termination	$1.3 \cdot 10^{10}$ L mol^{-1} s^{-1}	8.4 kJ mol^{-1}	$1.0 \cdot 10^{16}$ s^{-1}	280 kJ mol^{-1}
propagation with crosslinker	$1.6 \cdot 10^6$ L mol^{-1} s^{-1}	28.9 kJ mol^{-1}	$1.0 \cdot 10^9$ s^{-1}	83.7 kJ mol^{-1}
Crosslink reaction	$1.6 \cdot 10^6$ L mol^{-1} s^{-1}	28.9 kJ mol^{-1}	$1.0 \cdot 10^9$ s^{-1}	83.7 kJ mol^{-1}

b) Unimolecular to bimolecular reaction (as forward of the reversible):

The derivation for the apparent rate coefficients of these type of reactions is very similar to the type a) reactions, as it is the reverse reaction put in a different way.:

$$A \underset{k_{+chem*}}{\overset{k_{-chem*}}{\rightleftharpoons}} BC \underset{k_{+diff}}{\overset{k_{-diff}}{\rightleftharpoons}} B + C \quad \Leftrightarrow \quad A \underset{k_{+app}}{\overset{k_{-app}}{\rightleftharpoons}} B + C$$

The expression for the apparent rate coefficients are similar:

$$\frac{1}{k_{-app}} = \frac{1}{k_{-chem}} + \frac{K_{eq}}{k_{+diff}} \qquad (S7)$$

$$\frac{1}{k_{+app}} = \frac{1}{k_{+chem}} + \frac{1}{k_{+diff}} \qquad (S8)$$

In Table S3, the Arrhenius parameters for related k_{+chem} and k_{-chem} combinations are shown.

Table S3: Arrhenius parameters for k_{+chem*} and k_{-chem*}, unimolecular to bimolecular reactions[6].

Reaction	k_{+chem}		k_{-chem}	
	A	E_a	A	E_a
β-scission	$2.2 \cdot 10^5$ L mol^{-1} s^{-1}	17.9 kJ mol^{-1}	$1.0 \cdot 10^9$ s^{-1}	83.7 kJ mol^{-1}

c) Bimolecular to bimolecular reaction:

. The general form of these reactions is[8]:

$$A + B \underset{k_{f,-diff}}{\overset{k_{f,+diff}}{\rightleftharpoons}} AB \underset{k_{-chem*}}{\overset{k_{+chem*}}{\rightleftharpoons}} CD \underset{k_{r,+diff}}{\overset{k_{r,-diff}}{\rightleftharpoons}} C + D \Leftrightarrow A + B \underset{k_{-app}}{\overset{k_{+app}}{\rightleftharpoons}} C + D$$

The general expression for the observed reaction rate after assuming the quasi-steady approximation for the calculation of the concentration of the encounter pairs AB and CD is:

$$\frac{dC}{dt} = -k_{-app}[C][D] + k_{+app}[A][B]$$

With:

$$\frac{1}{k_{+app}} = \frac{1}{k_{f,+diff}} + \frac{1}{k_{+chem}} + \frac{1}{K_{eq} k_{r,+diff}} \qquad (S9)$$

$$\frac{1}{k_{-app}} = \frac{1}{k_{r+diff}} + \frac{1}{k_{-chem}} + \frac{K_{eq}}{k_{f,+diff}} \qquad (S10)$$

and:

$$K_{eq} = \frac{k_{f,+diff}}{k_{f,-diff}} \frac{k_{+chem*}}{k_{-chem*}} \frac{k_{r,-diff}}{k_{r,+diff}} = \frac{k_{+chem}}{k_{-chem}} \qquad (S11)$$

In Table S4, the Arrhenius parameters for related $k_{+\text{chem}}$ and $k_{-\text{chem}}$ combinations are shown.

Table S4: Arrhenius parameters for $k_{+\text{chem}}$ and $k_{-\text{chem}}$, bimolecular to bimolecular reactions[3,6,7,9]**.**

Reaction	$k_{+\text{chem}}$		$k_{-\text{chem}}$	
	A	E_a	A	E_a
H-abstraction of crosslinker molecule	4.0 . 10^2 L mol^{-1} s^{-1}	29 kJ mol^{-1}	4.0 . 10^2 L mol^{-1} s^{-1}	29 kJ mol^{-1}
H-abstraction peroxide radical	1.0 . 10^2 L mol^{-1} s^{-1}		4.7 . 10^1 L mol^{-1} s^{-1}	28.9 kJ mol^{-1}
Crosslink H-abstraction	4.0 . 10^2 L mol^{-1} s^{-1}	29 kJ mol^{-1}	4.0 . 10^1 L mol^{-1} s^{-1}	29 kJ mol^{-1}

In the equations above the term k_{diff} appears, which is the corresponding diffusion rate coefficient and a measure for the rate at which the two species diffuse toward each other. This contribution is calculated using the Smoluchowski model with the mutual diffusion coefficient approximated by the sum of the translational diffusion coefficients of the reactants. Assuming one (diffusion rate dominant) reactant (e.g. propagation with monomer M) one obtains:[10–15]

$$k_{M,diff} = 4\pi\sigma_p N_A D_M \qquad (S12)$$

Then σ_p is the propagation reaction distance, N_A the Avogadro number and D_M is the translational diffusion coefficient of reactant m. D_M can be determined by the equation:

$$D_M = D_{M,0}\, e^{-\frac{E_{a,M}}{RT}\left(-V_M^* M_{j,M} \frac{\frac{w_m}{M_{j,M}}+\frac{w_p}{M_{j,M}}}{V_{FH}/\lambda}\right)} \qquad (S13)$$

$$\text{with } \frac{V_{FH}}{\lambda} = w_m \frac{V_{FH,M}}{\lambda_M} + w_p \frac{V_{FH,p}}{\lambda_p} \qquad (S14)$$

$$\text{and } \frac{V_{FH,A}}{\lambda_A} = K_{1,A}\left(K_{2,A} - T_{g,A} + T\right) \qquad (S15)$$

Table S5: Parameters to enable the calculation of the diffusion rate coefficient for macromolecules.[2]

Parameter	Description	Value[16–18]
$D_{M,0}\ (m^2 s^{-1})$	Pre-exponential factor for diffusion	$1.27\ 10^{-7}$
$E_{a,M}\ (kJ\ mol^{-1})$	Activation energy for diffusion	2.137
$R\ (J\ mol^{-1}K^{-1})$	Universal gas constant	8.314
$T\ (K)$	Temperature	463
$w_m\ (-)$	Mass fraction of monomer	0
$w_p\ (-)$	Mass fraction of polymer	1
$V_m^*\ (m^3 kg^{-1})$	Specific critical hole free volume of monomer	$0.872\ 10^{-3}$
$K_{1,M}\ (m^3\ kg^{-1}\ K^{-1})$	Parameter for specific hole free volume polymer	$6.91\ 10^{-7}$
$K_{2,p} - T_{g,p}\ (K)$	Parameter for specific hole free volume polymer	-250.21
$M_{j,M}\ (g\ mol^{-1})$	Molar mass monomer	90.05[a]

[a]For the peroxide radicals and the crosslinking agent a $M_{j,M}$-value of 100 g mol^{-1} is considered.

For macrospecies the following scaling-law is adopted:[10–15]

$$D_i^{com} = \frac{D_M^{com}}{i^{0.664+2.02w_p}} \qquad (S16)$$

in wich w_p is the mass fraction of polymer, i the chain length of the polymer chain and D_m^{com} the center-of-mass diffusion coefficient. Simulations results showed that the exponent $0.664+2.02w_p$ underestimated the diffusion of polymer chains and thus is taken equal to a constant value of 2.15. The diffusional parameters employed in this study are shown in Table S5:

Another method for determining k_{diff} is the RAFT-CLD-T method developed by Johnston-Hall and Monteiro[19] which is essentially a superposition of different power laws (see Equation (9)-(13) in the main text).

The system-specific parameters are experimentally determined and are usually only valid for one monomer type and a singular temperature making their application range limited to the studied polymerization systems. Table S6 shows the parameters that were used in this study:

Table S6: RAFT-CLD-T parameters for the calculation of the $k_{t,app,ij}$.[2]

Temperature	i_{gel}	i_{SL}	α_s	α_l	α_{gel}	$log(k_{t,11})$
463 K	5.4 $w_p^{-2.51}$	30	0.31	0.31	0.95	8.25

S.3 References

1 M. Buback, B. Huckestein, F. -D Kuchta, G. T. Russell and E. Schmid, *Macromol. Chem. Phys.*, 1994, **195**, 2117–2140.

2 D. R. D'hooge, M. F. Reyniers and G. B. Marin, *Macromol. React. Eng.*, 2009, **3**, 185–209.

3 G. Arzamendi, C. Plessis, J. R. Leiza and J. M. Asua, *Macromol. theory simulations*, 2003, **12**, 315–324.

4 A. B. Vir, Y. W. Marien, P. H. M. Van Steenberge, C. Barner-Kowollik, M.-F. Reyniers, G. B. Marin and D. R. D'hooge, *React. Chem. Eng.*, 2018, **3**, 807–815.

5 G. Arzamendi, C. Plessis, J. R. Leiza and J. M. Asua, *Macromol. Theory Simulations*, 2003, **12**, 315–324.

6 A. B. Vir, Y. W. Marien, P. H. M. Van Steenberge, C. Barner-Kowollik, M.-F. Reyniers, G. B. Marin and D. R. D'hooge, *Polym. Chem.*, 2019, **10**, 4116–4125.

7 N. Ballard, S. Hamzehlou and J. M. Asua, *Macromolecules*, 2016, **49**, 5418–5426.

8 D. R. D'hooge, M. F. Reyniers and G. B. Marin, *Macromol. React. Eng.*, 2013, **7**, 362–379.

9 A. Snijder, B. Klumperman and R. Van Der Linde, *J. Polym. Sci. Part A Polym. Chem.*, 2002, **40**, 2350–2359.

10 M. C. Griffiths, J. Strauch, M. J. Monteiro and R. G. Gilbert, *Macromolecules*, 1998, **31**, 7835–7844.

11 J. Nicolas, L. Mueller, C. Dire, K. Matyjaszewski and B. Charleux, *Macromolecules*, 2009, **42**, 4470–4478.

12 J. S. Vrentas and C. M. Vrentas, *J. Polym. Sci. Part B Polym. Phys.*, 2003, **41**, 501–507.

13 J. S. Vrentas, J. L. Duda and H. C. Ling, *J. Polym. Sci. Part A-2, Polym. Phys.*, 1984, **22**, 459–469.

14 J. S. Vrentas and J. L. Duda, *J Polym Sci Polym Phys Ed*, 1977, **15**, 403–416.

15 M. V Smoluchowski, *Zeitschrift für Phys. Chemie*, , DOI:10.1017/CBO9781107415324.004.

16 D. R. D'hooge, M.-F. Reyniers and G. B. Marin, *Macromol. React. Eng.*, 2009, **3**, 185–209.

17 D. S. Achilias and C. Kiparissides, *Macromolecules*, 1992, **25**, 3739–3750.

18 D. S. Achilias, *Macromol. Theory Simulations*, 2007, **16**, 319–347.

19 M. J. M. GEOFFREY JOHNSTON-HALL, *J. Polym. Sci. Part A Polym. Chem.*, 2008, **49**, 511–512.